Calculating Asphaltenes Precipitation Onset Pressure by Using Cardanol as Precipitation Inhibitor: A Strategy to Increment the Oil Well Production

Camilo Andrés Guerrero-Martin, Universidade Federal do Rio de Janeiro – Instituto de Macromoléculas; Erik Montes-Páez, Universidad Industrial de Santander; Márcia Cristina Khalil de Oliveira, Petrobras; Jonathan Campos and Elizabete F. Lucas, Universidade Federal do Rio de Janeiro – Instituto de Macromoléculas

Abstract

Asphaltenes precipitation is considered a formation damage problem, which can reduce the oil recovery factor. It fouls piping and surface installations, as well as cause serious flow assurance complications and decline oil well production. Therefore, researchers have shown an interest in chemical treatments to control this phenomenon. The aim of this paper is to assess the asphaltenes precipitation onset of crude oils in the presence of cardanol, by titrating the crude with n-heptane. Moreover, based on this results obtained at atmosphere pressure, the asphaltenes precipitation onset pressure were calculated to predict asphaltenes precipitation in the reservoir, by using differential liberation and refractive index data of the oils.

The influence of cardanol concentration on the asphaltenes stabilization of three Brazilian crude oils samples (with similar API densities) was studied. Therefore, three formulations of cardanol were prepared: The formulations were added to the crude at 5:98, 1.5:98.5, 2:98 and 4:96 ratios.

The petroleum samples were characterized by API density, elemental analysis and differential liberation test. The asphaltenes precipitation onset was determined by titrating with n-heptane and monitoring with near-infrared (NIR). The asphaltenes precipitation onset pressures were estimated. The envelope phase of the crude oils were also determined by numerical simulation (pipesim). In addition, supported in the downhole well profile and a screening methodology, the adequate artificial lift systems (ALS) for the oils were selected. Finally, the oil flow rates were modelling by NODAL analysis production system in the SNAP software.

The results of this study show the refractive index for each sample, and the predictive pressure to asphaltene instability. The asphaltenes precipitation onset of the crude oils were 2.06, 2.30 and 6.02 mL of n-heptane/g of oil. The cardanol was an effective inhibitor of asphaltenes precipitation, since it displaces the precipitation pressure of the oil to lower values. This indicates that cardanol can increase the oil wells productivity.

Introduction

Petroleum can be subdivided into four fractions that can be identified by the SARA (Saturated, Aromatic, Resins and Asphaltenes) analysis. The asphaltenes fraction is the most complex to be characterized, because it consists of the heavier molecules of higher polarity and molecular structure composed of individual and/ or condensed aromatic rings. (Leon et al. 2012)

Several operational problems are associated with asphaltenes, which, due to variation in composition, pressure and temperature, can precipitate and subsequently form organic scales deposition in the porous media, pipelines, or surface facilities. The reservoir complications can be effective porosity losses, changes in the permeability, and wettability.(Jamaluddin et al. 2000; Asomaning et al. 2001; Martin C. A. G. & Páez, E. M. 2017)

Different kinds of chemicals have been tested to stabilize asphaltenes, but all experimental analyses are done under room temperature and atmospheric pressure. (Moreira et al. 1998; Moreira et al. 1999; Ferreira et al. (2015); Lucas et al. 2015; Figueira et al. 2017)

This work focused in the prediction of the onset precipitation pressure using the refraction index (RI) and a correlation proposed by Buckley J. S. et al, 2007 and increased production as a consequence of the application of cardanol as an asphaltene precipitation inhibitor.

Experimental Section Materials

Three Brazilian dead crude oil samples (Sample A, Sample B, Sample C) having different API gravities, asphaltenes precipitation onset, PVT test, SARA compositions, rheological information, refractive index (RI) measurements and wellbore data were donated by Petrobras. The samples were provided with the PVT data showed in Figure 1. Sample A recombination was pressurized to 5120 psi at 158 °F and bubble point pressure 3812 psi. Sample B recombination was pressurized to 5120 psi at 175.46 °F and bubble point pressure 3300 psi. Sample C recombination was pressurized to 8534 psi at 159.8 °F, bubble point pressure 4610 psi and thermal expansion coefficient of 8.2915×10^{-4} C^{-1}.

Methods and techniques

API gravities and SARA

The crude oils were characterized by the methodology based in the standard test method for relative density of oils by digital density analyzer DMA 4-500 Antom Par. Furthermore, the IATROSCAN MK-6 was used to determine the SARA composition aplicating the technical standard IP 469: *Determination of saturated, aromatic and polar compounds in petroleum products by thin layer chromatography and flame ionization detection.*

Asphaltenes precipitation onset

The asphaltenes precipitation onset was determined using Bruker MATRIX-F near-infrared (NIR) spectrophotometer system (Lucas E.F. et al., 2009; Garreto M. et al., 2013; Aguiar J. I. et al., 2014), operating with the Opus 6.5 software, connected to a Jasco PU 2087 Plus displacement pump.

Seven grams of pure crude oil was poured into the device's cup while kept under constant magnetic stirring. Then a probe with 5 mm optical path was introduced in the cup and the system was turned on simultaneously with the start of titration of the precipitant, at a flow of 0.1 mL/min.

the analysis was finalized AFTER 8 ½ hours and a graph was plotted of absorbance versus n-heptane volume, revealing the volume of n-heptane corresponding to the minimum absorbance point, indicating onset of asphaltenes precipitation.

The asphaltenes precipitation onset index (IP) was obtained by dividing the n-heptane volume by 7, since the onset is expressed in terms of mL of n-heptane/g of oil phase.

The cardanol (additive) was tested in three concentrations 0.10, 0.15 and 0.30 g in 7 g of crude oil, representing ratios of 1.5:98.5, 2:98 and 4:96 respectively. Furthermore, the test was carried out in duplicate and the result was expressed as the average value
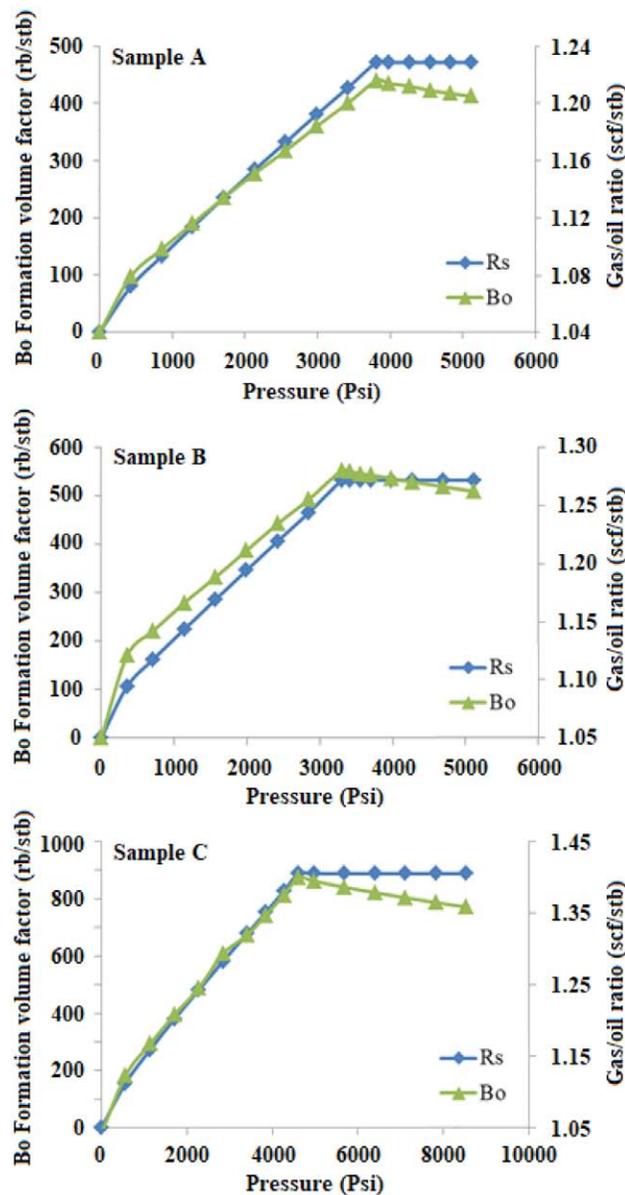

Figure 1—PVT data for samples A, B and C.

Rheology
The tests were carried out in in the modular advanced rheometer system HAAKE MARS. Varying the temperature and the shear rate.

Refractive index at standard conditions
A Michelson interferometer was used to measure refractive index at 25°C and 1 atm. n-Heptane 99.5% of purity from Isofar Co, was used to dilute the crude oil to 0.10, 0.20, 0.30, 0.40 and 0.45 %v/v. The measurement of the distance (δ) between the mirrors position with crude oil contained in a capillary tube and without the capillary tube, allowed determinate the oil refractive index (n_{Oil}). The Fig. 2 shows the schematic representation of the experiment.
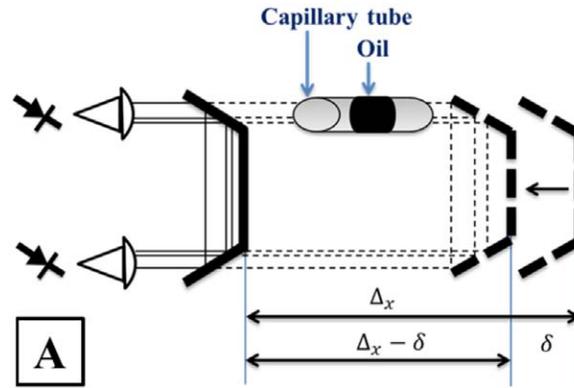
Figure 2—Schematic representation for the measurement of refractive index of crude oils.

The adjustment of the phase difference can estimate the quotient between the speed of light through the air (c_{air}) and the speed of light through the crude oil (c_{Oil}), calculated by using the Equation 1. Where, l_{Oil} is the length of the oil in the capillary tube.

$$n_{Oil} = \frac{c_{air}}{c_{Oil}} = 1 + \frac{2\delta}{l_{oil}} \qquad \text{(Eq. 1)}$$

Calculation of RI at reservoir conditions from PVT DATA

In 1998, Buckley and collaborators presented the Eq. 2 that permits to predict the asphaltenes instability tendency at any pressure. The mathematical expression correlates the refractive index (n) at standard conditions, dimensionless, with reservoir fluid properties, gas/oil ratio (R_s), scf/stb, and the formation volume factor (B_o), rb/stb. The molar fraction (x_i) of the light end components (C_1, C_2, C_3), dimensionless, and their molar refractions (R_i), cm³/mol, were also involved.

$$\left(\frac{n^2-1}{n^2+2}\right)_{\text{Live oil}} = \frac{1}{B_o}\left(\frac{n^2-1}{n^2+2}\right)_{\text{STO}}^0 + 7.52 \times 10^{-6}\frac{R_s}{B_o}\sum_i x_i R_i \qquad \text{(Eq. 2)}$$

The purpose of the Eq. 2 was calculate, from PVT data and measured RI for standard conditions, the RI of live oil. (Buckley J. S. et al. 2007) The prediction of precipitation onset pressure is the point at the intersection of the live oil RI curve and the P_{RI}, which is defined as the refractive index of the mixture of n-heptane/oil required to start asphaltenes precipitation. (Wang & Buckley, 2001; Buckley J. S. et al. 1998)

Crude oil phase envelope at reservoir conditions

The phase envelope plots at reservoir conditions were done in the commercial software *Pipesim®* using PVT data, rheological data and SARA composition.

Wellbore data, Artificial lift system (ALS) screening, and production estimate

The studied reservoir is characterized by the ultra-deep depths and high pressures. For the production modeling were selected the Well A-Sample A and the Well B-Sample B.

The Appendix 1 presents an example of a well summary report. The drilling depth was 23056.29 ft. and presented a side track at 3552.099 ft (Appendix) maximum angle of 22.05° and the Verticalization of the well occurred at 17372.93ft. On top of that, was described a simple completion at 23024,006 ft. The mud weight window (MWW) varied between 110 gr/cc and 140 gr/cc. well tests indicate the potential flow rates of 600-7600 Bbl./d per well.

The dogleg severity it's defined as "*the measure of the change in direction of a well bore over a defined length, normally measured in degrees per 100 feet of lengt"h,* and calculated by the Eq. 3.

$$\cos(\text{Previous Inclination}) \times \cos(\text{Current Inclination}) = A$$
$$\sin(\text{Previous Inclination}) \times \sin(\text{Current Inclination}) = B$$
$$\cos(\text{Change in azimut}) = C$$
$$A + (B \times C) = D$$
$$\frac{\cos^{-1}(D)}{D \times \frac{\text{Well L. (m)}}{30}}$$

(Eq 3)

The methodology for selection the most adequate ALS was made taking into account the most important operational parameters for each system, like: number of wells, reservoir temperature, initial reservoir pressure, completion type, and others.

To estimate the production gain when the flowing pressure (Pwf) drops caused by the addition of the maximum additive concentration (0.30 g Cardanol) was used the nodal analysis method performed in the SNAP software of the Rydder Scott company. The node of the analysis was in the reservoir and the inflow performance relationship (IPR) was constructed by vogel equation.

Results and discussion

API gravities and SARA compositions of crude oils
The specifications of the crude oils are shown in the Table 1.

Table 1—API and Sara compositions for each crude oil sample.

Samples name	API	Saturates	Aromatics	Resins	Asphaltenes
Sample A	17.68	18.17	30.31	30.62	20.88
Sample B	23.93	22.74	38.63	18.15	20.46
Sample C	24.98	26.05	32.21	27.22	14.49

Rheological information
Rheological behavior of the samples is showed in the Table 2. The Sample B presented a high dynamic viscosity η attributed by oil composition.

Table 2—Rheological details for the crude oil samples.

Oil sample	Temperature °F	Shear rate (1/s)	η Dynamic viscosity (mPa.s)
Sample A	140	10 50 80 120 250	107 108 108 108 109
Sample B	140	10 50 80 120 250	143.35 143.43 143.65 145.87 151.35
Sample C	140	10 50 80 120 250	33 33 33 33 35

Refractive index

According to the RI behavior of the crude oil dilutions can be linearized their growth trend. The Fig. 3 presents the RI the P_{RI} for each oil.
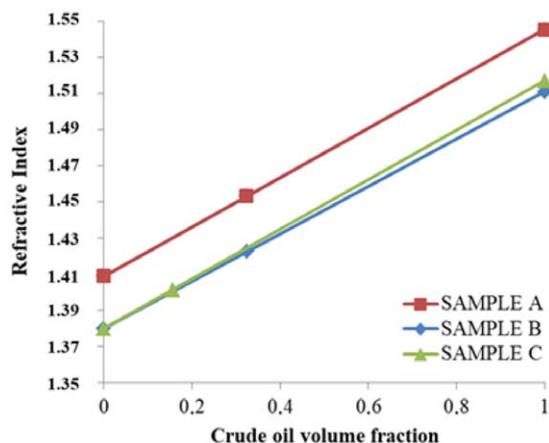

Figure 3—Refractive index correlation for Samples A, B and C.

Cardanol performance as asphaltenes precipitation inhibitor

The directly use of the Cardanol in the oil sample caused asphaltenes stabilization, that was evidenced in the increment of n-heptane amount that be required to induce the asphaltenes precipitation. (see Table 3)

Table 3—Precipitacion index for the crude oil samples.

Samples	Precipitation Index (PI)			
	Pure crude oil	Cardanol 0.10 g	Cardanol 0.15 g	Cardanol 0.30 g
Sample A	**2.06**	2.60	2.746	3.362
Sample B	**2.30**	2.92	3.139	3.624
Sample C	**6.02**	7.100	7.114	7.132

In the sample A the addition of 0.10 g of cardanol displacement the pressure precipitation onset from 7759 to 6265 psi, 0.15 and 0.30 g of cardanol situate the pressure in 5910 and 4589 psi respectively (Fig. 4a). For the oil sample B the precipitation onset pressure reduces from 7080 psia to 5240, 4816 and 3438 for each additive concentration 0.10, 0.15, 0.30 g. The oil sample C (Fig. 4c), not presented a severe asphaltenes instability.
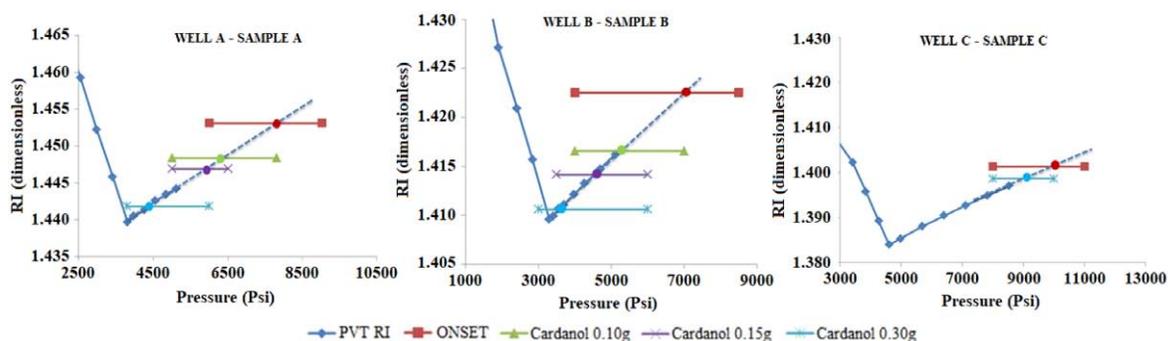

Figure 4—Behavior of the RI versus pressure of each crude oil and the P_{RI} obtained for 0.10, 0.15 and 0.30 grams of cardanol.

Crude oil phase envelope at reservoir conditions

Fig. 5a, 5b, 5c. The graphics indicates that samples are from a black oil reservoir. The reservoir has a satisfactory petrophisical properties, the producer formation has an average thickness of 80 feet and the initial water saturation at the reservoir was 17%. Depth conditions and initial pressure were estimated at 22500ft and 8350 psi for both wells. The CO_2 concentration of the Well A-Sample A is close to 0.42 of the total gases. The complete information for the light ends associated to the three crude oils is reported in the Appendix A-1 and Appendix A-2.
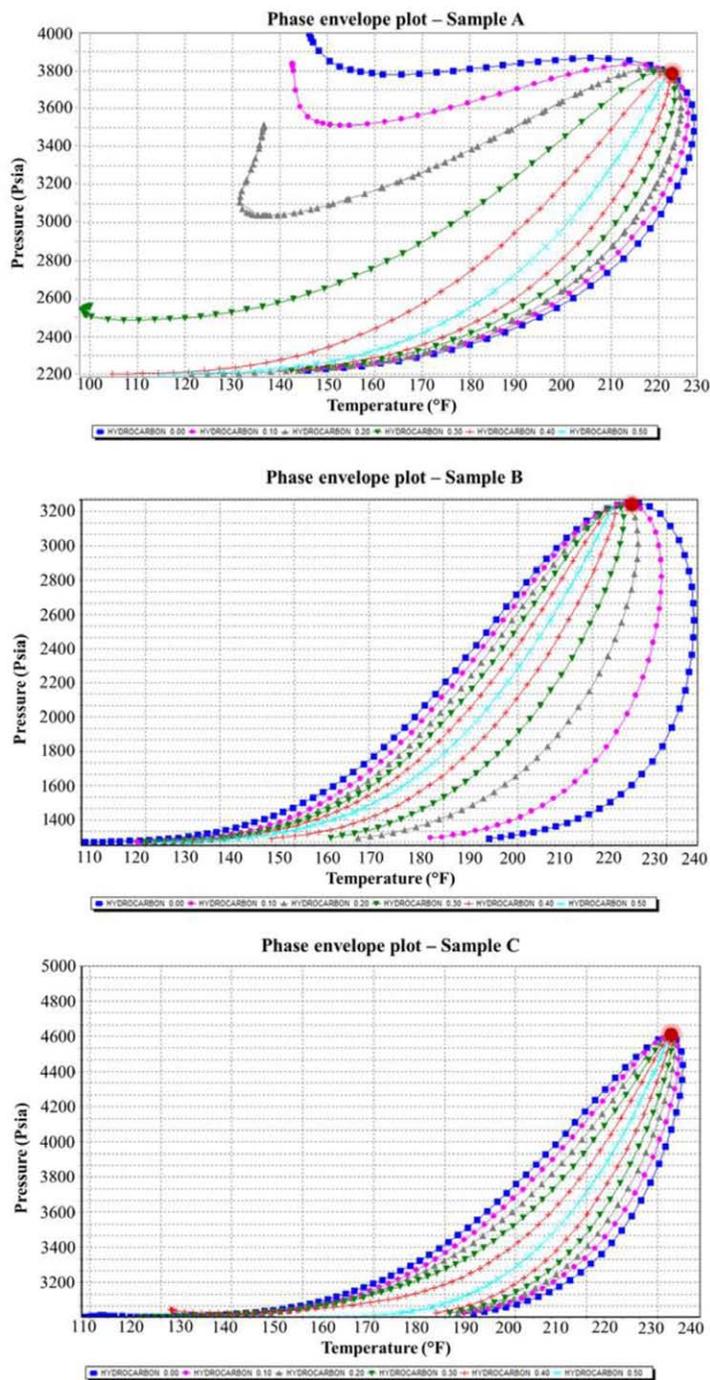

Figure 5—Phase envelope plot of each sample.

ALS selection and nodal Analysis.

The ALS selection methodology gave the Jet pump as the most effective. The localization, depth and temperature were the parameters that determinate the choice. (Fig 6a, 6b)

The recommended pump was manufactured by *Oilmaster*, works with a water power fluid with 1500 – 70000 psi fluid pressure and parallel tubing strings with gas vented at 50%. The pump depth is 16530 ft at true vertical depth (TVD).
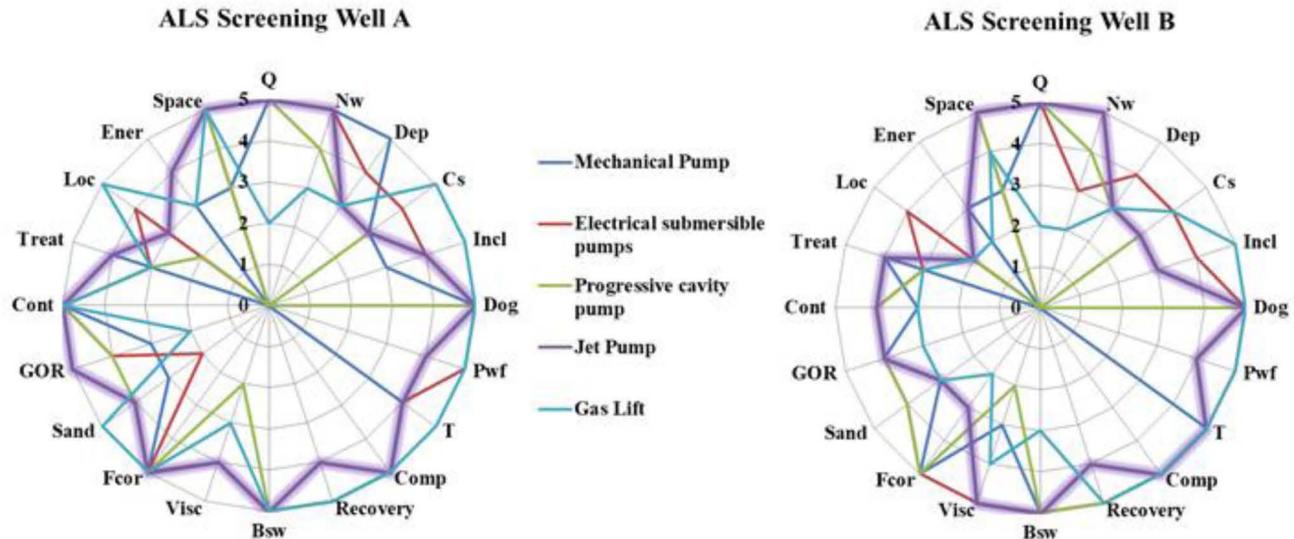

Figure 6—Artificial lift Selection methodology for the Well A and the Well B.

The nodal analysis was performed or the oils with asphaltenes instability: Sample A and sample B. In the Well A-Sample A the reduction of the Pwf produced an incremental production of 3600 stb/d. (See Fig. 7a, 7b) For the case of the well B-sample B lower the Pwf represents 5350 new barrels. (See Fig. 8a, 8b) The positive values obtained for the new oil production rates confirm the effective of the cardanol as asphaltenes precipitation additive.
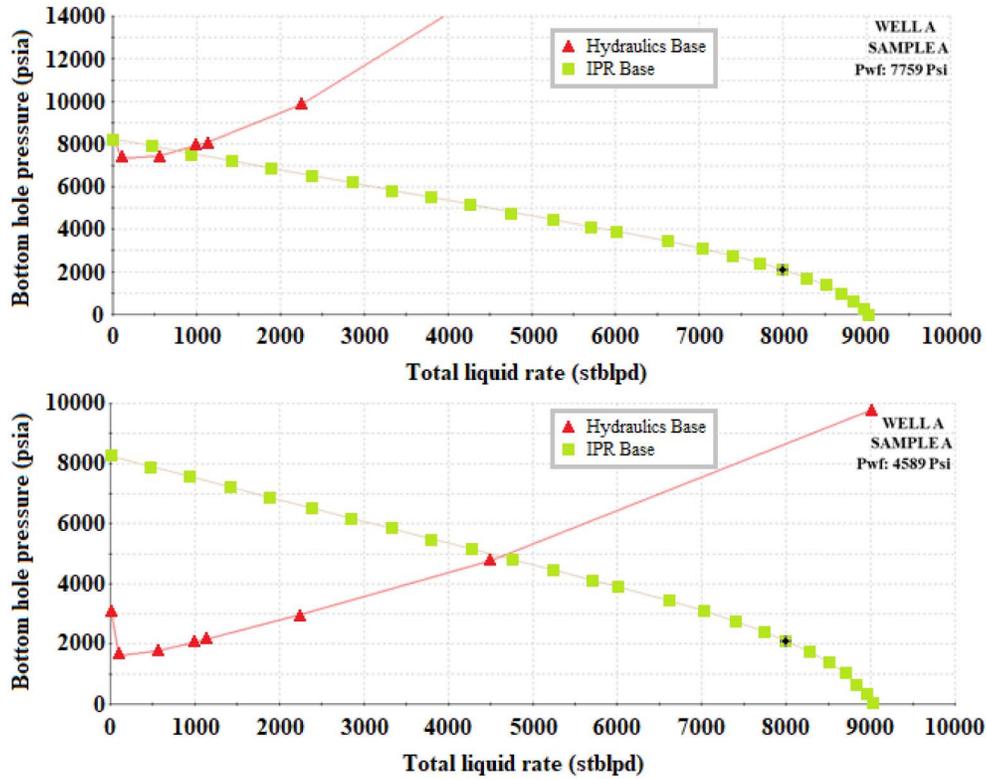
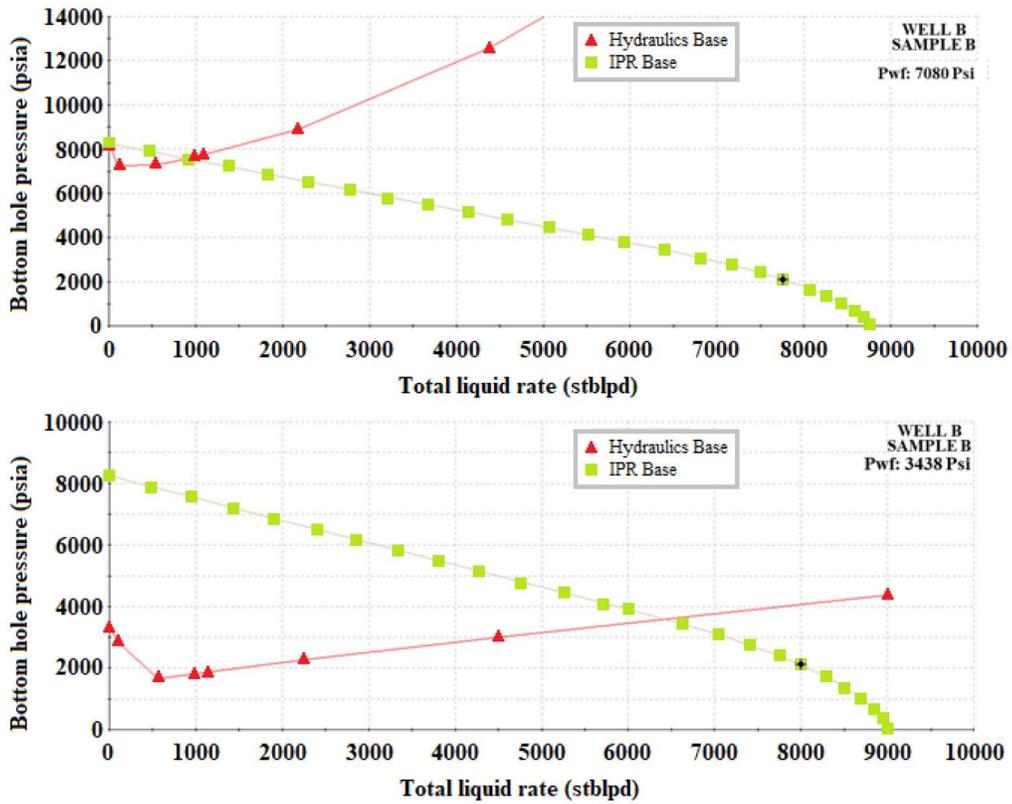Figure 7—Nodal analysis for the Well A, variations the Pwf.

Figure 8—Nodal analysis for the Well B, variations the Pwf.

Conclusions

The refractive index of the crude oils dilutions presented a linear behavior and the results of this work can be used for oil samples with similar characteristics.

The equation proposed by Buckley et al, 2007 allowed the correct prediction of precipitation pressure of asphaltenes.

The cardanol is an optimal inhibitor of asphaltene precipitation and can be used in industrial scale to reduce these problems. The production rate was drastically increases; neverthless the economic viability should be studied.
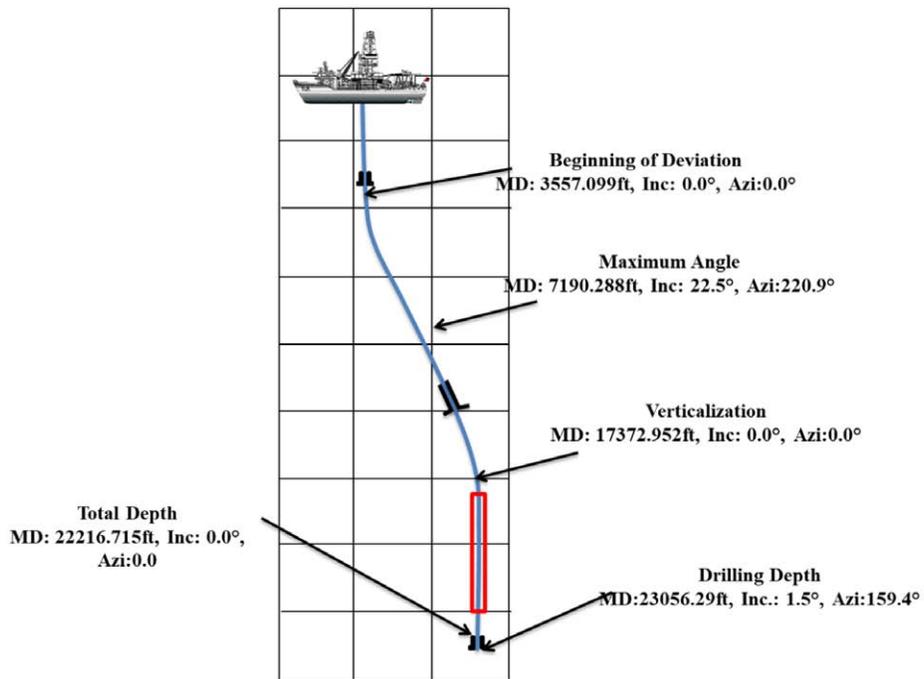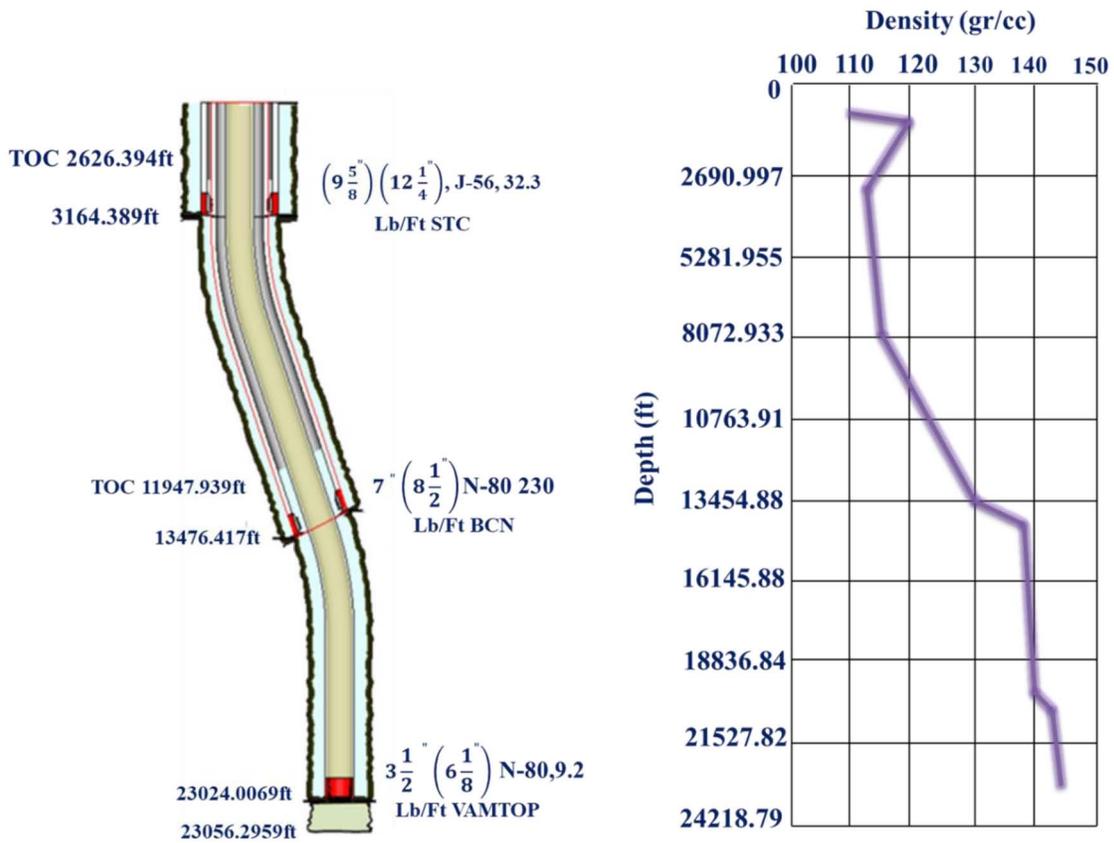
Acknowledgements

References

Aguiar, J. I., Garreto, M. S., Gonzaáez, G., Lucas, E. F., & Mansur, C. R. (2013). Microcalorimetry as a new technique for experimental study of solubility parameters of crude oil and asphaltenes. *Energy & Fuels*, **28**(1), 409–416.

Asomaning, S. (2003). Test methods for determining asphaltene stability in crude oils. *Petroleum Science and Technology*, **21**(3-4), 581–590.

Buckley, J. S., Hirasaki, G. J., Liu, Y., Von Drasek, S., Wang, J., & Gill, B. S. (1998). Asphaltene precipitation and solvent properties of crude oils. *Petroleum Science and Technology*, **16**(3-4), 251–285.

Ferreira, S. R., Louzada, H. F., Moyano-Dip, R. M., Gonzalez, G., & Lucas, E. F. (2015). Influence of the architecture of additives on the stabilization of asphaltenes and water-in-oil emulsions separation. *Energy & Fuels*, **29** (11), 7213–7220.

Figueira, J. N., Simão, R. A., Soares, B. G., & Lucas, E. F. (2017). The influence of chemicals on asphaltenes precipitation: a comparison between atomic force microscopy and near infrared techniques. *REVISTA FUENTES*, **15**(1), 7–17.

Garreto, M. S. E., Mansur, C. R. E., & Lucas, E. F. (2013). A model system to assess the phase behavior of asphaltenes in crude oil. *Fuel*, **113**, 318–322.

IP – 469 Standard Maethod. *Determination of saturated, aromatic and polar compounds in petroleum products by thin layer chromatography and flame ionization detection.*

Jamaluddin, A. K. M., Joshi, N., Joseph, M. T., D'Cruz, D., Ross, B., Creek, J., & McFadden, J. D. (2000, June). Laboratory techniques to define the asphaltene precipitation envelope. In petroleum society's Canadian international petroleum conference in Calgary, Canada.

León, E. A., Quintero, J. F. G., Cervantes, A. A. B., & Rangel, E. R. S. (2012). Análisis de la simulación de precipitación de asfaltenos en el crudo del campo Colorado. *REVISTA FUENTES*, **10**(1).

Lucas, E. F., Mansur, C. R., Spinelli, L., & Queirós, Y. G. (2009). Polymer science applied to petroleum production. *Pure and Applied Chemistry*, **81**(3), 473–494.

Lucas, E. F., Ferreira, L. S., & Khalil, C. N. (2015). Polymers Applications in Petroleum Production. *In: Encyclopedia of Polymer Science and Technology*. Mark, H. F. (ed.). John Wiley & Sons, Inc. 1–50.

Martin, C. A. G., & Páez, E. M. (2017). Efeito da salinidade na tensão interfacial do sistema óleo/agua em condições isobáricas e incremento gradual da temperatura. *REVISTA FUENTES*, **15**(2), 117–124.

Moreira, L. F. B., González, G., & Lucas, E. F. (1998). Estudo da interatividade entre macromoléculas asfaltênicas e compostos estabilizantes: LCC e cardanol. *Polímeros: Ciência e Tecnologia* **VIII**(3), 46–54.

Moreira, L. F. B., González, G., & Lucas, E. F. (1999). Stabilization of asphaltenes by phenolic compounds extracted from cashew-nut shell liquid. *Journal of Applied Polymer Science*, **73**(1), 29–34 (1999)

Wang, J. X., & Buckley, J. S. (2001, January). An experimental approach to prediction of asphaltene flocculation. In SPE International Symposium on Oilfield Chemistry. Society of Petroleum Engineers.

Appendix A

Downhole well profile, MWM and graphic report of the directional drilling.

TOC 2626.394ft

3164.389ft

$\left(9\frac{5}{8}"\right)\left(12\frac{1}{4}"\right)$, J-56, 32.3
Lb/Ft STC

TOC 11947.939ft

13476.417ft

$7"\left(8\frac{1}{2}"\right)$N-80 230
Lb/Ft BCN

$3\frac{1}{2}"\left(6\frac{1}{8}"\right)$N-80,9.2
Lb/Ft VAMTOP

23024.0069ft

23056.2959ft

Density (gr/cc)

Depth (ft)

Beginning of Deviation
MD: 3557.099ft, Inc: 0.0°, Azi:0.0°

Maximum Angle
MD: 7190.288ft, Inc: 22.5°, Azi:220.9°

Verticalization
MD: 17372.952ft, Inc: 0.0°, Azi:0.0°

Total Depth
MD: 22216.715ft, Inc: 0.0°,
Azi:0.0

Drilling Depth
MD:23056.29ft, Inc.: 1.5°, Azi:159.4°

Appendix B

Ligth ends fractions for Samples A, B and C

SAMPLES	Ligth ends fractions			
	CO_2	C_1	C_2	C_3
SAMPLE A	0.42	0.11	0.013	0.02
SAMPLE B	0.13	0.46	0.46	0.36
SAMPLE C	0.37	0.34	0.49	0.34